

Anatomical Properties and Near Infrared Spectra Characteristics of Four *Shorea* Species from Indonesia

Danang Sudarwoko Adi^{1*}, Sung-Wook Hwang², Dwi Ajas Pramasari¹, Yusup Amin¹, Hairi Cipta³, Ratih Damayanti⁴, Wahyu Dwianto^{1*}, Junji Sugiyama^{2,5}

¹Research Center for Biomaterials, Indonesian Institute of Sciences, Cibinong Science Center, Bogor, Indonesia

²RISH, Kyoto University, Gokasho, Uji, Kyoto, Japan

³Gajah Mada University, Yogyakarta, Indonesia

⁴Forest Product Research and Development Center, Indonesian Ministry of Environment and Forestry, Bogor, Indonesia

⁵College of Materials Science and Engineering, Nanjing Forestry University, Nanjing, China

ARTICLE INFO

Article history:

Received October 10, 2019

Received in revised form June 1, 2020

Accepted June 14, 2020

KEYWORDS:

Shorea wood,
Near-infrared,
Anatomical properties,
PCA, k-NN

ABSTRACT

This study investigated the anatomical properties and absorbance characteristics of NIR spectra of four *Shorea* species from Indonesia. Macroscopic section revealed that Balau has similarity with Heavy Red Meranti, whereas White Meranti was almost identical with Light Red Meranti. All of the woods have diffuse porous and axial resin canals in tangential lines at the microscopic level. Original NIR spectra of *Shorea* species showed different absorbance characteristic. Wood density was assumed to be one of the factors that affected to the absorbances. Principal component analysis (PCA) of second derivative NIR spectra at the wavenumber 8,000-4,000 cm⁻¹ (full) and 6,200-5,600 cm⁻¹ (specific) showed different orientation among the Principal Component (PC) number. PC1, which contained highest spectral variation, had two closed clusters (1) Balau and Heavy Red Meranti and (2) White and Light Red Meranti at full spectral range. In contrast, the results at specific range were (1) Balau and White Meranti and (2) Heavy and Light Red Meranti. Hierarchical clustering dendrogram using PCA data from two spectral regions resulted in two types of clustering, the 8,000-4,000 cm⁻¹ was somehow related to 'density', while the 6,200-5,600 cm⁻¹ was grouped in 'color' information from visual inspection. From both spectral regions, k-nearest neighbour (k-NN) classification models revealed 100% accuracy in identification four *Shorea* species using NIR spectra.

1. Introduction

Shorea wood, well known as "Meranti", is one of the important timber trade in Indonesia, with about 10% of the total volume of wood log production (Statistics of Forestry Production 2017). It is classified as the first group of the commercial wood due to its high economic value and categorized into 6 main timber trade groups such as Yellow Meranti, White Meranti, Red Meranti, Balau, Red Balau, and Bangkirai (Decree of The Minister of Forestry 2003). There are many species which are included in each group. For instance, Red Meranti has around 15 species, like *Shorea uliginosa*, *S. parvifolia*, *S. leprosula*, *S. selanusa*, *S. palembanica* (Martawijaya *et al.* 2005). In addition, genera of *Shorea* consists of 194 species, which is

distributed from Sri Lanka and India through Indo-China towards Malesia (Soerianegara and Lemmens 1994). In Indonesia, it is common to use a local name in the wood market. In addition, the name is also based on the weight of the wood. For example, Red Meranti has two major names, which are called Light and Heavy Red Meranti (Soerianegara and Lemmens 1994). The difference between these two groups is the density of wood.

It is common that wood of different species may vary widely in appearance, such as color, texture, and figure. There are also variability in the cell patterns produced by different combinations and factors like size, arrangement, and alignment, (Panshin and de Zeeuw 1980). These properties, which generally called anatomical properties, are important to distinguish and identify the wood species. However, there are also possibilities that some species may have

* Corresponding Author

E-mail Address: danang@biomaterial.lipi.go.id

similarity of these features. For instance, (Hwang et al. 2016) revealed that *Pinus densiflora* for. *erecta* and *Pinus silveris* have similar anatomical features, thus it was difficult to determine the differences between two species.

Identification of Indonesian *Shorea* species still used conventional approaches, such as uses macroscopic and microscopic methods to see the anatomical features. Since they come from the same genera, some species of *Shorea* may have identical anatomical properties, therefore distinguish of each species is challenging. Moreover, traditional methods for wood identification are time and labour consuming because they include the use of physical, anatomical, and visual inspections (Yang et al. 2015). Therefore, the application of the other technique for *Shorea* identification is also required to obtain the result faster and simple.

One of the other method for wood identification is using near infrared (NIR) spectroscopy. This technique with an aid of chemometrics is useful not only for quantification but also for qualification (Tsuchikawa and Kobori 2015). NIR spectroscopy utilizes the spectral range of near infrared between $12,820\text{ cm}^{-1}$ and $4,000\text{ cm}^{-1}$ in wavenumber or 780 and 2,500 nm in wavelength (Schwanninger et al. 2011), where overtone vibration of functional groups are observable. Application of the NIR spectra for wood discrimination or classification has been successful to distinguish the difference between species (Tsuchikawa et al. 2003; Pastore et al. 2011; Yang et al. 2015; Abe et al. 2016; Lang et al. 2017; Ramalho et al. 2018; Ma et al. 2019). Furthermore, this technique also provides good results to distinguish species in the same genera (Gierlinger et al. 2004; Espinoza et al. 2012; Horikawa et al. 2015; Hwang et al. 2016).

In this study, four wood species from similar genera of *Shorea*, which are common in Indonesia's wood market, were investigated to distinguish the anatomical properties and to know the appearance of these wood species to the NIR spectra. In Indonesia timber trade, every local group names of the wood such as Red Meranti, White Meranti, and Balau have different prices and qualities. Furthermore, identification of the sawn wood in the market is a problematic for the consumers because due to weathering and other factors wood decolorization makes identification more complicated. In such situations, the aimed of this study was to show the benefit of NIR technique for wood identification in the

genera of *Shorea* in comparison with the commonly method.

2. Materials and Methods

2.1. Materials

This study used four *Shorea* species, which were taken from wood collection in Xylarium Bogoriense-Indonesia. The local timber trade names are Heavy Red Meranti, Light Red Meranti, White Meranti, and Balau. All of the wood samples were in the genera of *Shorea*. Eleven wood blocks were prepared from each species to obtain the NIR spectra and microscopy samples, where the size of the wood blocks was $2 \times 2 \times 2$ cm, in longitudinal (l), tangential (t) and radial (r) respectively. In addition, the average wood density was also determined for each species based on the wet volume (Miranda et al. 2011).

2.2. Anatomical Analysis

Microscopic sections were used to observe the anatomical features. Wood sections were cut in tangential, radial and cross section by a sliding microtome, with a thickness of $15\ \mu\text{m}$. The sections were stained with safranin solution, followed by dehydration with graded ethanol series, and finally mounted on the glass slides. Then, the image of each section were captured with a light microscope (Olympus BX-51) equipped with digital camera (Olympus DP 73). In addition, the stereo micrographs of the cross section were also obtained. Identification under the microscopy level was conducted based on the IAWA list for hardwood species (Wheeler et al. 1989).

2.3. Near-Infrared Spectroscopy Analysis

The longitudinal-radial (LR) of wood blocks were subjected to obtain the near-infrared (NIR) spectra (Perkin Elmer Spectrum 100N). Both sides of the LR face were scanned. In average, 22 spectra were measured from each species. The spectra were collected at the wavenumber of $10,000\text{--}4,000\text{ cm}^{-1}$ with a spectral resolution of 16 cm^{-1} , and 32 scans per each record process. The original spectra were second derivatived by Savitzky-Golay filter smoothing to nine points with third order function (Savitzky and Golay 1964). For principal component analysis, the spectral region over $8,000\text{ cm}^{-1}$, which was considered to be non-informative due to noise, was excluded from the analysis.

2.4. Multivariate Data Analysis and Classification Models

In principal component analysis (PCA), a total of 20 partial spectral regions were tested to investigate the selective effects of the NIR spectra as well as the full length of 8,000–4,000 cm^{-1} . An unsupervised hierarchical clustering was performed by the agglomerative Ward's minimum variance method. It was shown as a dendrogram to represent the numerical distances between the data. The classification of the four *Shorea* species were conducted with k-nearest neighbour (k-NN) algorithm. The training and test sets were randomly selected at a ratio of 0.75 to 0.25, respectively. All programming related to NIR spectrometric analysis, including data processing and PCA, was done by Python version 3.7.

3. Results

3.1. Anatomical Properties

Figure 1 showed the macroscopic and microscopic features of White Meranti. Anatomical observation based on the IAWA standard for hardwood species revealed that the wood has characteristics as follows: 2. Growth ring boundaries indistinct or absent; 5. Wood diffuse-porous; 7. Vessels in diagonal and/or radial pattern; 43. $\geq 200 \mu\text{m}$ (mean tangential diameter of vessel lumina); 44. $207 \pm 22 \mu\text{m}$ (mean tangential diameter of vessel lumina); 46. ≤ 5 vessels per square millimeter; 79. Axial parenchyma vascentric; 80. Axial parenchyma aliform; 82. Axial parenchyma winged-aliform; 83. Axial parenchyma confluent; 92. Four (3–4) cells per parenchyma strand; 97. Ray width 1 to 3 cells; 98. Larger rays commonly 4- to 10-seriate; 102. Ray height $>1 \text{ mm}$; 104. Body ray cells procumbent with one row of upright and/or square marginal cells; 105. 4–12 /mm (Rays per mm); 128. Axial resin canals in long tangential lines.

Anatomical features on Figure 2 showed that the characteristics of Light Red Meranti were: 2. Growth ring boundaries indistinct or absent; 5. Wood diffuse-porous; 7. Vessels in diagonal and/or radial pattern; 9. Vessels exclusively solitary (90% or more); 42. 100–200 μm (Mean tangential diameter of vessel lumina); 44. $162 \pm 37 \mu\text{m}$ (Mean tangential diameter of vessel

lumen); 47. 5–20 vessels per square millimeter; 79. Axial parenchyma vascentric; 80. Axial parenchyma aliform; 92. Four (3–4) cells per parenchyma strand; 97. Ray width 1 to 3 cells; 104. 4–12 /mm (Rays per mm); 127. Axial resin canals in long tangential lines; 128. Axial canals in short tangential lines.

Figure 3 shows the anatomical properties of Heavy Red Meranti. The features shows that the characteristics were: 2. Growth ring boundaries indistinct or absent; 5. Wood diffuse-porous; 7. Vessels in diagonal and/or radial pattern; 43. $\geq 200 \text{ m}$ (Mean tangential diameter of vessel lumina); 44. $307 \pm 42 \mu\text{m}$ (Mean tangential diameter of vessel lumina); 46. ≤ 5 vessels per square millimeter (Vessel per square millimeter); 79. Axial parenchyma vascentric; 86. Axial parenchyma in narrow bands or lines up to three cells wide; 93. Eight (5–8) cells per parenchyma strand; 98. Larger rays commonly 4- to 10-seriate; 97. Ray width 1 to 3 cells; 103. Rays of two distinct sizes; 102. Ray height $>1 \text{ mm}$; 104. $\leq 4 \text{ /mm}$ (Rays per mm); 127. Axial canals in long tangential lines; 128. Axial canals in short tangential lines.

Figure 4 showed the anatomical features of Balau. It shows that this species has: 2. Growth ring boundaries indistinct or absent; 5. Wood diffuse-porous; 7. Vessels in diagonal and/or radial pattern; 10. Vessels in radial multiples of 4 or more common; 42. 100–200 μm (Mean tangential diameter of vessel lumina); 44. $183 \pm 35 \mu\text{m}$ (Mean tangential diameter of vessel lumina); 47. 5–20 vessels per square millimeter; 79. Axial parenchyma vascentric; 82. Axial parenchyma winged-aliform; 93. Eight (5–8) cells per parenchyma strand; 97. Ray width 1 to 3 cells; 98. Larger rays commonly 4- to 10-seriate; 104. 4–12 /mm (Rays per mm); 128. Axial canals in short tangential lines.

3.2. NIR Spectra Analysis

Figure 5 showed the original spectra of *Shorea* woods. The response of those species to the NIR absorbance was difference. It was clearly seen that the highest absorbance was Balau, followed by Heavy Red Meranti, White Meranti, and Light Red Meranti, respectively. However, the differences of original spectra among these species were almost similar, thus, it was difficult to distinguish the important peak of wood samples.

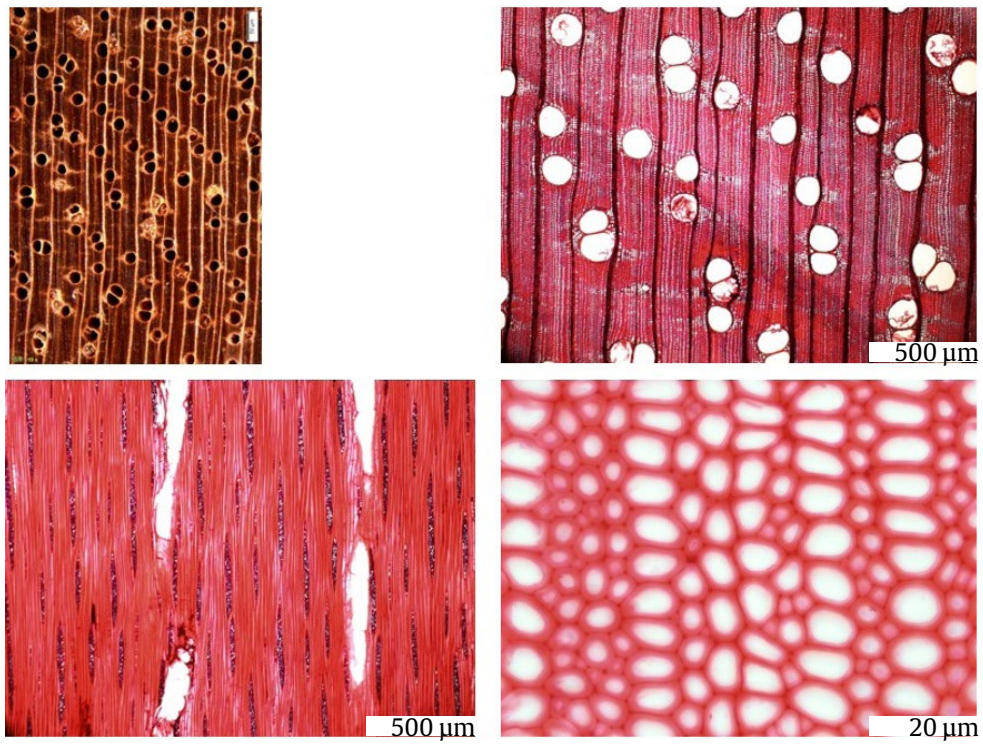


Figure 1. Macroscopic and microscopic sections of White Meranti

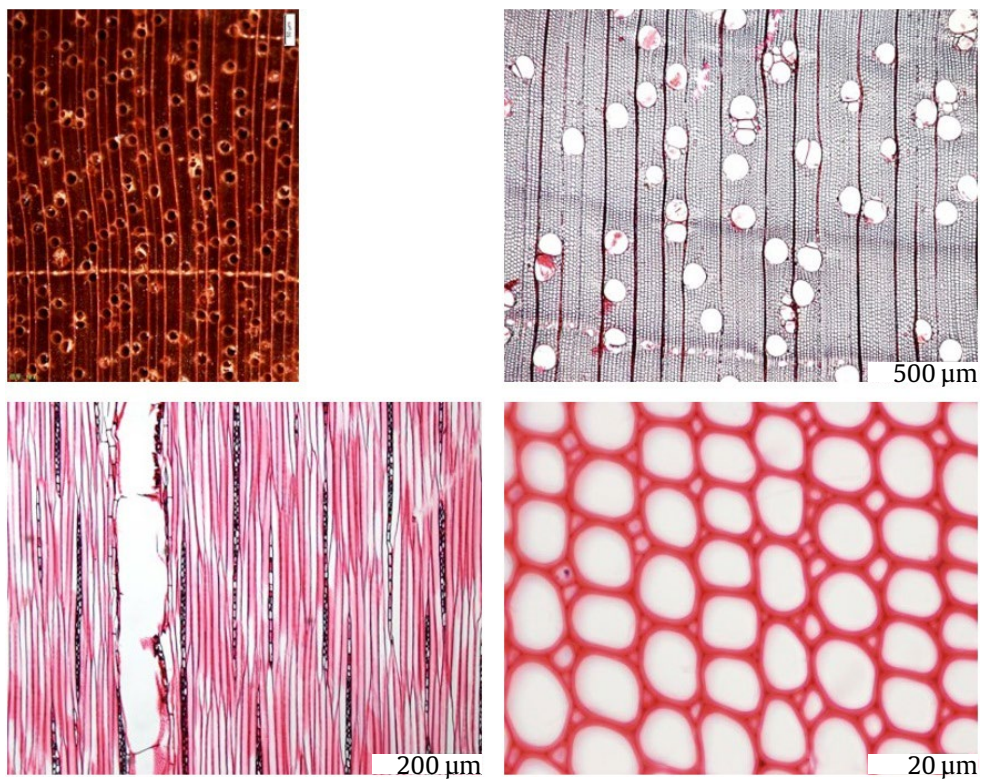


Figure 2. Macroscopic and microscopic sections of Light Red Meranti

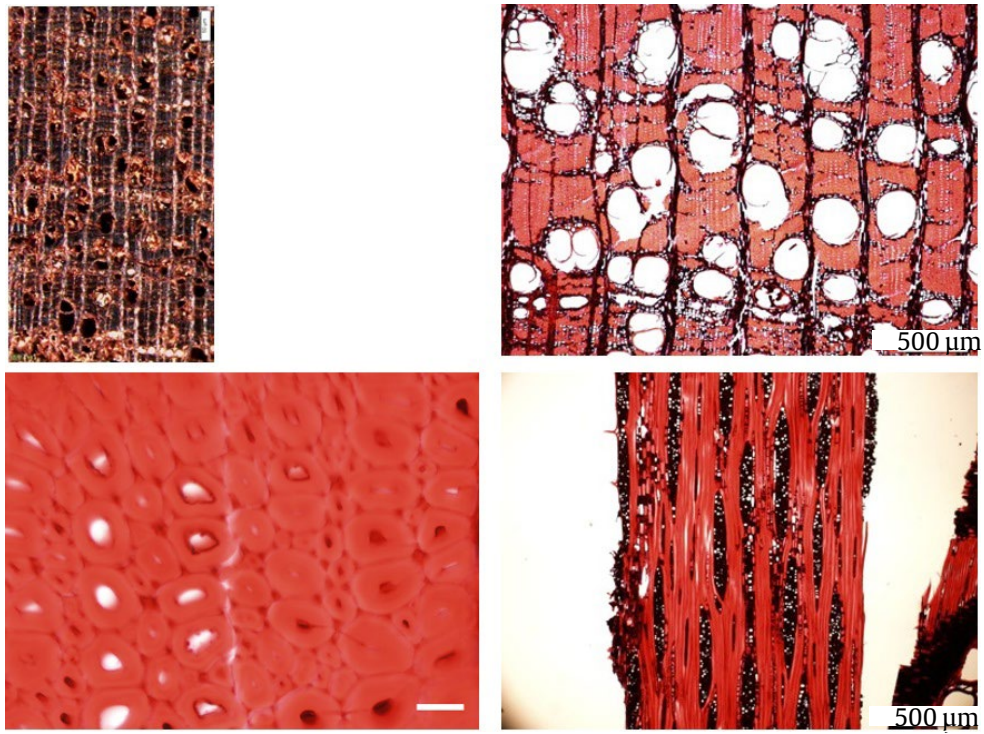


Figure 3. Macroscopic and microscopic sections of Heavy Red Meranti

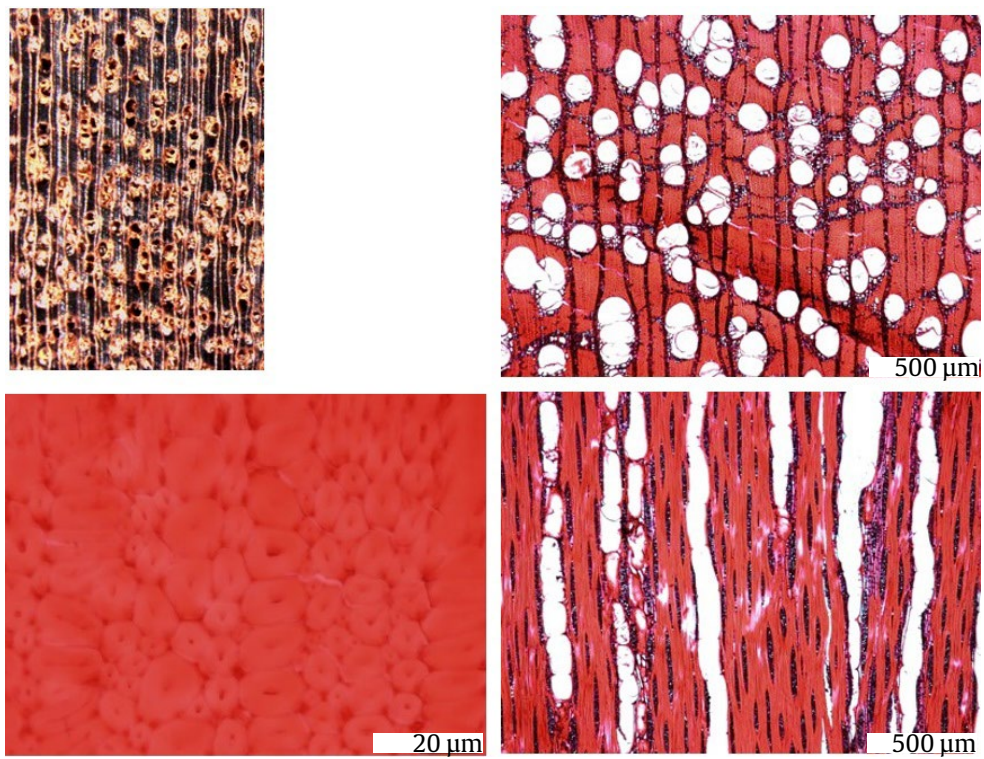


Figure 4. Macroscopic and microscopic sections of Balau

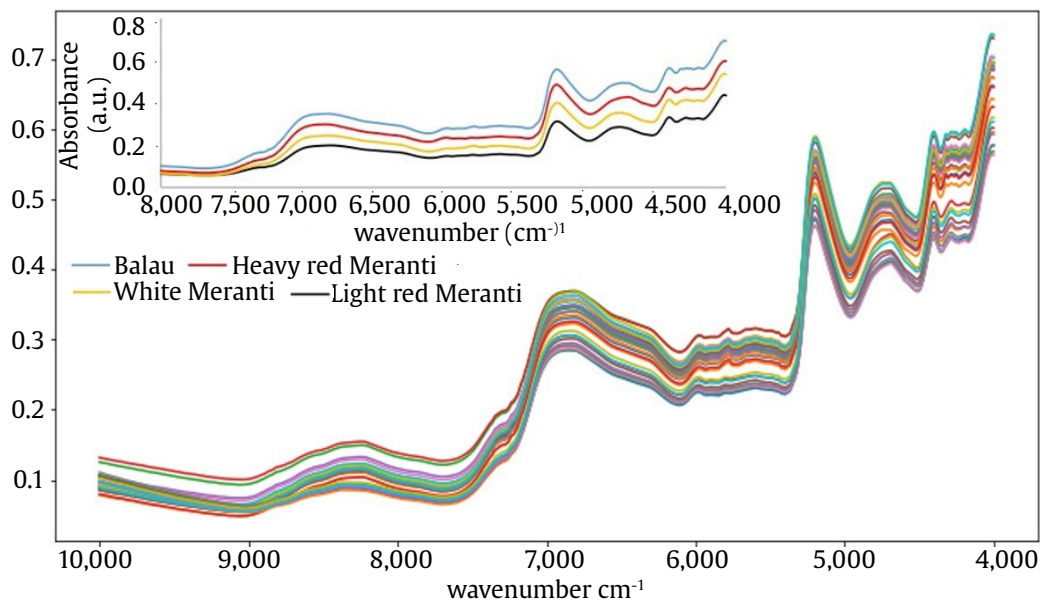


Figure 5. Original spectra of all the samples at wavenumber 10,000–4,000 cm^{-1}

3.3. PCA Analysis

The three sub-figures in Figure 6 present the PCA score plot and PC loadings on the first two principal components and the second derivative NIR spectra of the *Shorea* species in the 8,000–4,000 cm^{-1} spectral region, respectively. In the score plot, the four *Shorea* species created their own clusters that were clearly distinguished for both PC1 and PC2 (Figure 6a). PC loading spectra (Figure 6b) provided us with information on which NIR absorption bands contribute to such a clear distinction in the score plot.

Of the twenty spectral regions systematically tested, the 6,200–5,600 cm^{-1} showed a different aspect from the others. In the PCA score plot in this region, the four *Shorea* species were clearly clustered (Figure 7a), with high contributions at the 5,800 cm^{-1} band assigned to furanose or pyranose due to hemicellulose on PC1 and 5,980 cm^{-1} assigned to aromatic skeletal due to lignin on PC2 (Figure 7b).

4. Discussion

White Meranti differ from Red Meranti by their color (whitish-brown) and more numerous vessels (Soerianegara and Lemmens 1994), however, identifying based on the color is not a simple because the color may have changed due to weather, time, environment, etc. In addition, the density is higher, which is 0.54 g/cm^3 compare to 0.27 g/cm^3 . Light Red Meranti has a density of 0.25 to 0.45 g/cm^3 (Bosman et al. 1994). Figure 1 and 2 show that the fiber wall of White Meranti was thicker than Light Red Meranti. Moreover, the frequency of the tip cell in the White Meranti was also higher. It indicated that the fiber of

White Meranti might had long of fiber length. Honjo et al. (2006) stated that the greater the frequency of the tip cell, the longer the wood fiber was.

Heavy Red Meranti differ from Balau by its lower density and less numerous rays (Soerianegara and Lemmens 1994). However, Figure 3 shows that rays cell in the Heavy Red Meranti was wider than Balau. The density in this study were 0.64 g/cm^3 and 0.76 g/cm^3 , respectively. The wall thickness is believed as one of the factor affect the density. Figure 3 and 4 show that the fiber cell in Balau was thicker (wall thickness) and smaller (diameter) than the Heavy Red Meranti. Even, the lumen of the fiber cell in Balau species was very small and almost closed. Martawijaya et al. (2005) proposed that Balau species has a density between 0.88 g/cm^3 (*Shorea sumatrana*) to 1.04 g/cm^3 (*S. falcifera*).

Although conventional method through analysis of anatomical features has been successful to identify the four *Shorea* wood in this study, this method needs an extra effort to prepare the sample. The result was also take a time. Every *Shorea* group on the Indonesian timber market has many species, thus, comparing macroscopic and microscopic features of all the group for specific purposes are labour intensive. This study was conducted with limited wood sample of every *Shorea* group to give preliminary information of the wood response when subjected to the NIR spectra.

The original spectra showed baseline difference, but no differentiation according species was seen (Gierlinger et al. 2004). The absorbance characteristics affected by density. It meant the higher the density, the higher the absorbance was (Via et al. 2012). The wood samples with high density has small light scattering patterns

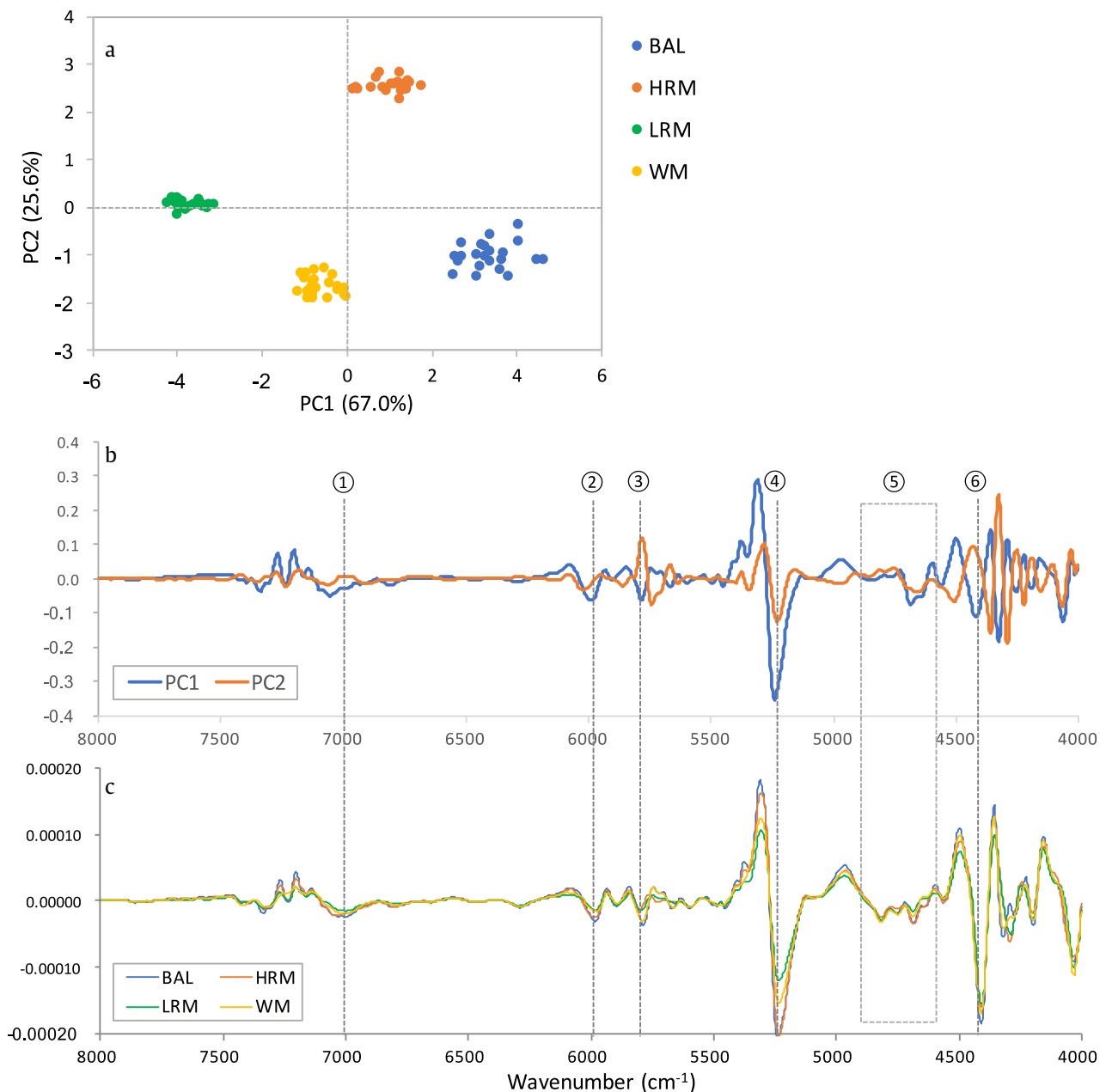


Figure 6. The PCA score plot (a) and loading spectra, (b) of the first two principal components and the second derivative NIR spectra of the four *Shorea* species, (c) in the 8,000-4,000 cm^{-1} spectral region. Encircled numbers represent the absorption bands assigned to the major wood components with high PC loading values. (1) 7,000 cm^{-1} , the amorphous regions in cellulose; (2) 5,980 cm^{-1} , aromatic skeletal due to lignin; (3) 5,800 cm^{-1} , furanose or pyranoside due to hemicellulose; (4) 5,220 cm^{-1} , water; (5) 4,890–4,620 cm^{-1} , cellulose; (6) 4,404 cm^{-1} , cellulose and hemicellulose. BAL, Balau; HRM, Heavy Red Meranti; LRM, Light Red Meranti; WM, White Meranti

(Ma *et al.* 2019). Whereas, in the second derivative spectra (Figure 6c), some differences were revealed at the absorption bands that assigned to representative wood components.

The purpose of PCA is to decompose the data matrix and concentrate the source of variability in the data into first few PCs (Hori and Sugiyama 2003). In addition, it was used to reveal a spectral range that leads to the sharpest

low-dimensional projection to find clusters (Gierlinger *et al.* 2004). We found six absorption bands representing the spectral differences in the second derivative NIR spectra with high PC loading values. PC1 loading showed the highest peak with a negative value at the 5,220 cm^{-1} band assigned to water. Indeed, this absorption band showed distinct differences between the *Shorea* species (Figure 8). In the water band (encircled four in

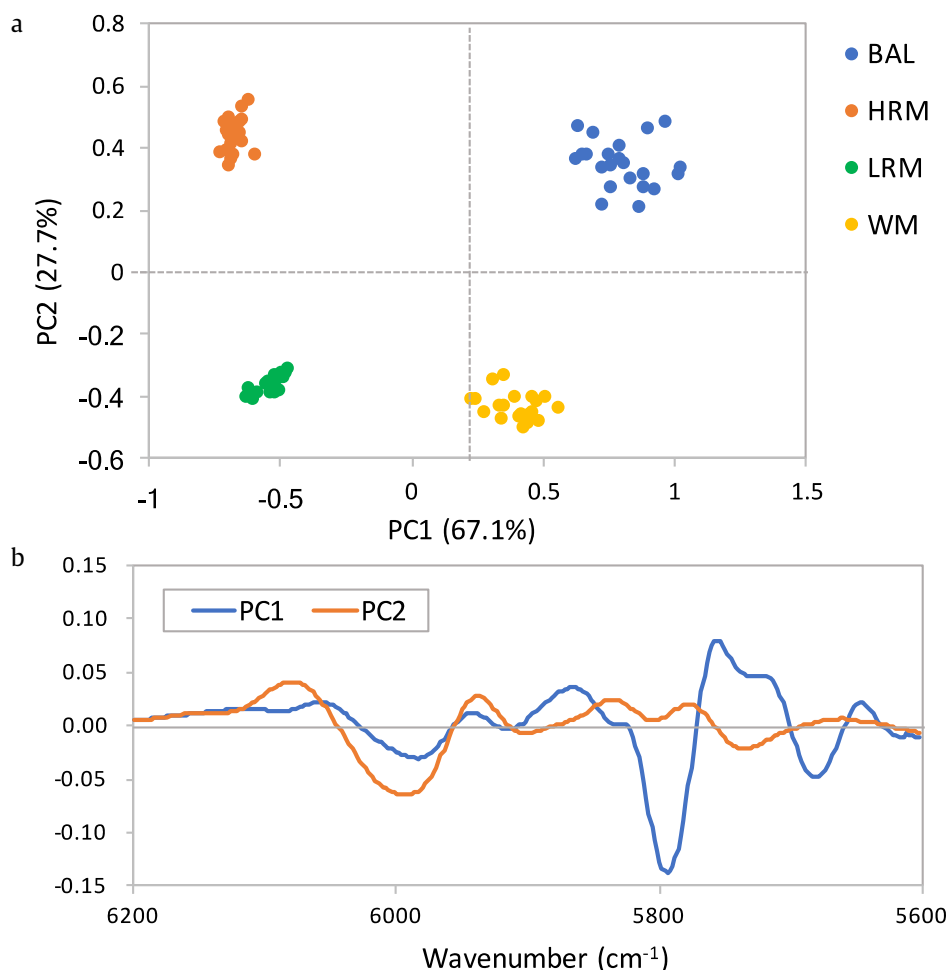


Figure 7. The PCA score plot (a) and loading spectra (b) on the first two principal components in the 6,200-5,600 cm^{-1} spectral region. BAL:Balau, HRM:Heavy Red Meranti, LRM:Light Red Meranti, WM:White Meranti

Figure 8), Balau and Heavy Red Meranti have stronger peaks than others, which contributed to their position in the positive area for the PC1 axis in the score plot. In this study, we used the second derivative NIR spectra, so the contribution of PC loadings in the score plot was interpreted in the opposite direction for each PC axis. There were some other notable bands, but they were not as dominant as the water.

For PC2 loading, the contribution of the 5,800 cm^{-1} band assigned to furanose or pyranose due to hemicellulose was prominent with a positive value. In this band, Balau and White Meranti indicated stronger intensity than others (encircled three in Figure 8), which contributed to their position in the negative area for the PC2 axis in the score plot. In addition, absorption bands such as 7,000 cm^{-1} assigned to amorphous regions in cellulose, 5,980 cm^{-1} aromatic skeletal due to lignin, 4,890-4,620 cm^{-1} cellulose, and 4,404 cm^{-1} cellulose and hemicellulose also showed relatively high values in both PC1 and PC2 loadings.

An interesting aspect that distinguished this short spectral region from others was revealed in the

hierarchical clustering analysis. Hierarchical clustering created two sub-clusters in all spectral regions tested. In most regions, including the 8,000-4,000 cm^{-1} , Light Red Meranti and White Meranti formed one cluster, while Heavy Red Meranti and Balau formed another (Figure 9a). Whereas, in the 6,200-5,600 cm^{-1} region only, two clusters were formed by pairing Light Red Meranti and Heavy Red Meranti, and Balau and White Meranti, respectively (Figure 9b). Although the lignin and hemicellulose-related wood components were the major differences that distinguished the four *Shorea* species, it was also noteworthy that the clustering result presented in the dendrogram in Figure 9b was consistent with the color similarity between them. In general, wood color was closely related to various extractives. It was not known at the moment, which wood extractives affect the color of the *Shorea* species, but the dendrogram suggested that wood color-related information may be hidden within the NIR spectral region of 6,200-5,600 cm^{-1} .

The identification result of the *Shorea* species using the k-NN classifier are presented in Figure 10 as a normalized

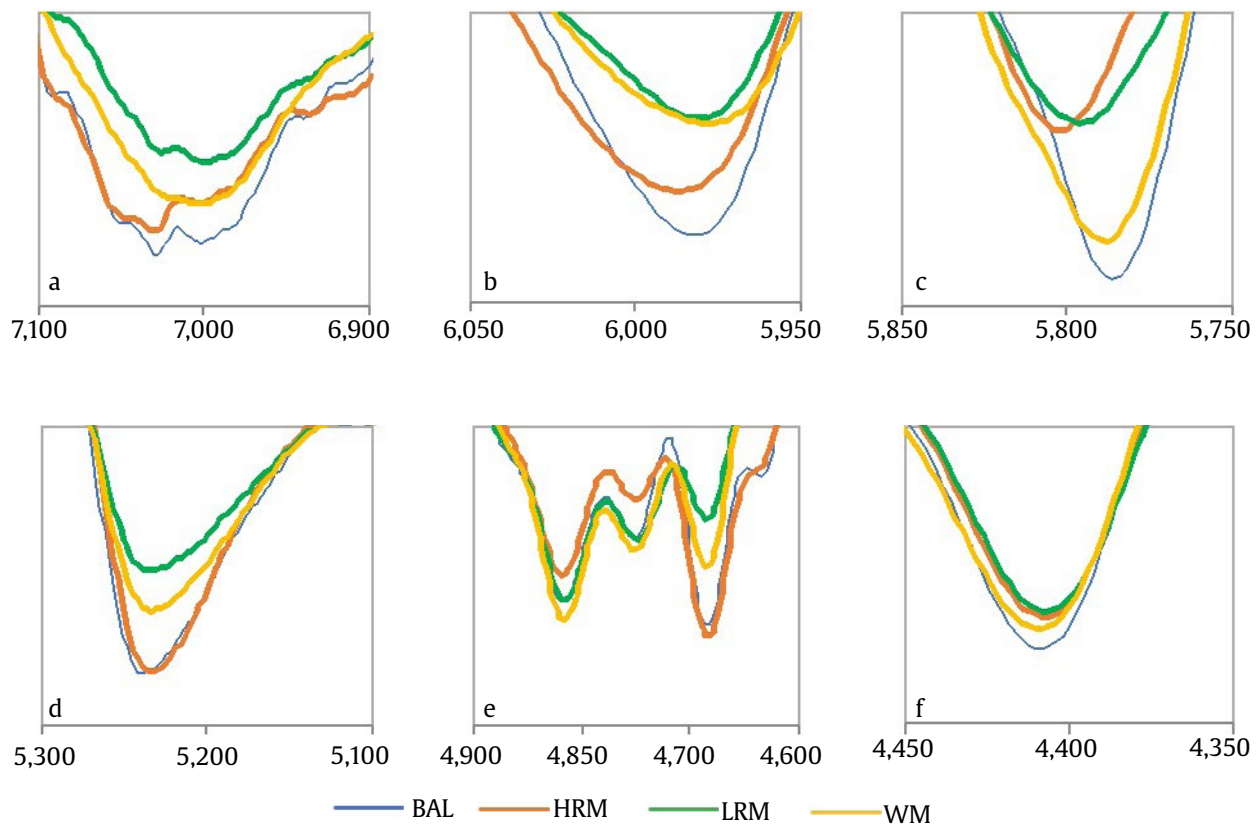


Figure 8. Enlarged spectra of the NIR spectral bands assigned to the major wood components presented in Figure 6. (a) 7,000 cm^{-1} , the amorphous regions in cellulose, (b) 5,980 cm^{-1} , aromatic skeletal due to lignin, (c) 5,800 cm^{-1} , furanose or pyranose due to hemicellulose, (d) 5,220 cm^{-1} , water; (e) 4,890–4,620 cm^{-1} , cellulose; (f) 4404 cm^{-1} , cellulose and hemicellulose. BAL:Balau, HRM:Heavy Red Meranti, LRM:Light Red Meranti, WM:White Meranti

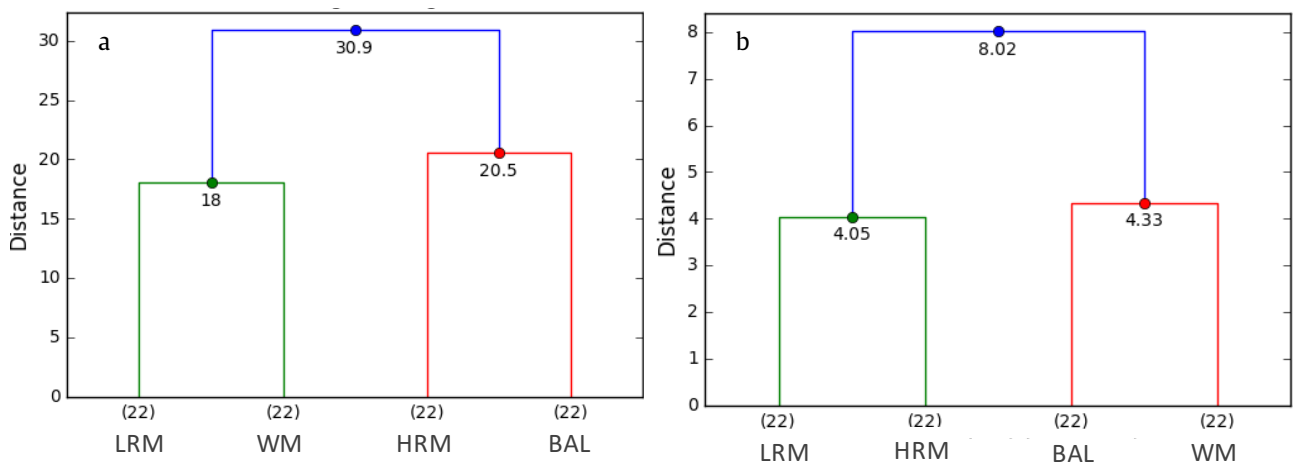


Figure 9. (a) Dendrograms of the four *Shorea* species in the two NIR spectral regions tested; 8,000–4,000 cm^{-1} , and (b) 6,200–5,600 cm^{-1} . The dendrograms are truncated to the top four cluster levels. The numbers in parentheses are the cluster size and the numbers at the junctions of the branches indicate the Euclidean distance between the clusters. BAL:Balau, HRM:Heavy Red Meranti, LRM:Light Red Meranti, WM:White Meranti

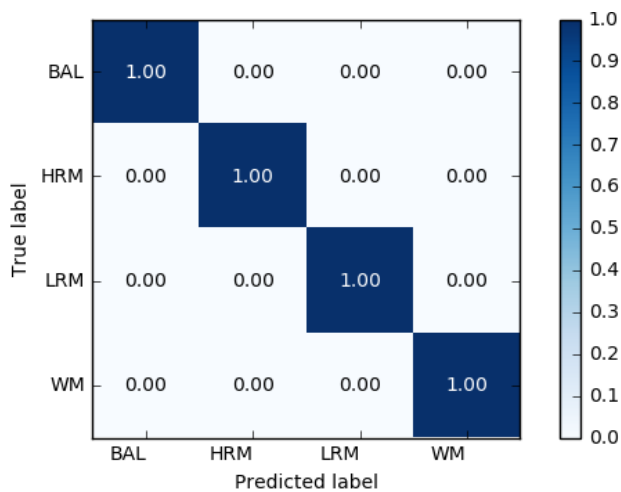


Figure 10. Normalized confusion matrix on the test set in the k-NN classification model ($k=3$). The test data are the second derivative NIR spectra with $8,000\text{--}4,000\text{ cm}^{-1}$ spectral region. The k-NN model produced the same result in the $6,200\text{--}5,600\text{ cm}^{-1}$. BAL:Balau, HRM:Heavy Red Meranti, LRM:Light Red Meranti, WM:White Meranti

confusion matrix. The k-NN classification model perfectly identified the *Shorea* species not only in the $8,000\text{--}4,000\text{ cm}^{-1}$ region but also in the $6,200\text{--}5,600\text{ cm}^{-1}$ region. As confirmed in the PCA results, the four *Shorea* species had significantly different characteristics in the NIR spectra. Since the possibility of *Shorea* identification based on chemical composition has been demonstrated from this study, the NIR chemometric approach may complement the conventional identification by visual inspection. The classification model will be more robust if the database contains a wide diversity within and between the *Shorea* species with a larger number of samples.

5. Conclusion

The macroscopic features of the Balau in this study was closely like Heavy Red Meranti, while the White Meranti was almost similar to the Light Red Meranti. At the microscopic level, all of the species have diffuse porous and axial canals in tangential lines. These are common properties in the genera of *Shorea*, thus, identification and classification of the *Shorea* wood was not easy. The highest density of the wood was Balau, followed by Heavy Red Meranti, White Meranti, and Light Red Meranti, respectively. The cell wall thickness and lumen diameter of the fiber were the factors, which affects the density. The

lumen of fiber cell in Balau was relatively closed, but the opposite result was found in Light Red Meranti.

The characteristics of these species were different when subjected to NIR analyses. The absorbance of the NIR spectra differs considerably among samples. The PCA analysis from two different spectral regions of $8,000\text{--}4,000\text{ cm}^{-1}$ and $6,200\text{--}5,600\text{ cm}^{-1}$, was found best in terms of classification of four *Shorea* species.

As explained, the precise and facile identification method for four commercially important *Shorea* species using NIR chemometrics was successfully introduced. However, the model was established from only four *Shorea* species so that it should be considered as preliminary. In order to make our model more robust and applicable even in non-professional market, it is prerequisite to make a database including a wide variety within and between the *Shorea* species.

Acknowledgements

The author (Danang S. Adi) would like to thank to the Ministry of Research, Technology and Higher Education of Indonesia, who give a scholarship for his study at Kyoto University through Research Innovation in Science and Technology Project (Riset-Pro). Taking data and sending the wood sample to RISH-Kyoto University is also partially supported by Japan-ASEAN Science, Technology and Innovation Platform (JASTIP) under the activity of the Strategic International Collaborative Research Program (SICORP), sponsored by Japan Science and Technology Agency (JST).

References

- Abe H et al. 2016. Simple separation of *Torreya nucifera* and *Chamaecyparis obtusa* wood using portable visible and near-infrared spectrophotometry: differences in light-conducting properties. *Journal of Wood Science* 62:210–212.
- Bosman MTM et al. 1994. Radial variation in wood properties of naturally and plantation grown light red Meranti (*Shorea*, Dipterocarpaceae). *IAWA Journal* 15:111–120.
- Decree of The Minister of Forestry. 2003. Decree of The Minister of Forestry of Indonesia No. 163/Kpts-II/2003. Available at: <http://arsip.rimbawan.com/images/stories/aturan-pdf/163 Kpts-II 2003.pdf>. [Data accessed: 1 September 2019]
- Espinoza JA et al. 2012. The potential use of near infrared spectroscopy to discriminate between different pine species and their hybrids. *Journal of Near Infrared Spectroscopy* 20:437–447.

- Gierlinger N *et al.* 2004. Characteristics and classification of Fourier-transform near infrared spectra of the heartwood of different larch species (*Larix* sp.). *Journal of Near Infrared Spectroscopy* 12:113–119.
- Honjo K *et al.* 2006. Introduction and verification of a novel method for measuring wood fiber length using a single cross section in *Acacia mangium*. *Trees - Structure and Function* 20:356–362.
- Horikawa Y *et al.* 2015. Near-infrared spectroscopy as a potential method for identification of anatomically similar Japanese diploxylons. *Journal of Wood Science* 61:251–261.
- Hwang S *et al.* 2016. Identification of Pinus species related to historic architecture in Korea using NIR chemometric approaches. *Journal of Wood Science* 62:156–167.
- Lang C *et al.* 2017. Discrimination of taxonomic identity at species, genus and family levels using Fourier Transformed Near-Infrared Spectroscopy (FT-NIR). *Forest Ecology and Management* 406:219–227.
- Ma T *et al.* 2019. Rapid identification of wood species by near-infrared spatially resolved spectroscopy (NIR-SRS) based on hyperspectral imaging (HSI). *Holzforchung* 73:323–330.
- Martawijaya A *et al.* 2005. Atlas kayu Indonesia Jilid I. Balai Penelitian dan Pengembangan Kehutanan. Departemen Kehutanan.
- Miranda *et al.* 2011. Wood properties of teak (*Tectona grandis*) from a mature unmanaged stand in East Timor. *Journal of Wood Science* 57:171–178.
- Panshin AJ, de Zeeuw C. 1980. *Textbook of Wood Technology. Structure, identification, properties, and uses of the commercial woods of the United States and Canada.* 4th ed. New York:Mc Grw-Hill Company.
- Pastore TCM *et al.* 2011. Near infrared spectroscopy (NIRS) as a potential tool for monitoring trade of similar woods: Discrimination of true mahogany, cedar, andiroba, and curupixá. *Holzforchung* 65:73–80.
- Ramalho FMG *et al.* 2018. Rapid discrimination of wood species from native forest and plantations using near infrared spectroscopy. *Forest System* 27:e008. DOI: 10.5424/fs/2018272-12075
- Savitzky A, Golay M J E 1964. Smoothing and differentiation of data by simplified least squares procedures. *Anal Chem* 36:1627–1639.
- Schwanninger M *et al.* 2011. A review of band assignments in near infrared spectra of wood and wood. *J Near Infrared Spectroscopy* 19:287–308.
- Soerianegara I, Lemmens RHMJInRHM. 1994. Prosea, plant resources of South-East Asia 5. Lemmens (Eds.). Timber trees: Major commercial timbers. Prosea, Bogor.
- Statistics of Forestry Production. 2017. Statistics of Forestry Production 2017. BPS-Statistics Indonesia. Available at: www.bps.go.id/publication/download [Date accessed: 29 August 2019]
- Tsuchikawa S, Kobori H. 2015. A review of recent application of near infrared spectroscopy to wood science and technology. *Journal of Wood Science* 61:213–220.
- Tsuchikawa S *et al.* 2003. Discriminant analysis of wood-based materials using near-infrared spectroscopy. *Journal of Wood Science* 49:275–280.
- Via B *et al.* 2012. Nonlinear multivariate modeling of strand density from near-infrared spectra. *Wood Science and Technology* 46:1073–1084.
- Wheeler EA. 1989. *Iawa List of Microscopic Features for Hardwood Identification.* Iawa Bulletin (Vol. 10). Leiden: IAWA.
- Yang *et al.* 2015. Preliminary investigation into the identification of wood species from different locations by near infrared spectroscopy. *BioResources* 10: 8505–8517.